Proceedings of the 11th Australasian Heat and Mass Transfer Conference, AHMTC11

9-10th July 2018, RMIT University, Melbourne, Australia

Put paper number here

CHARACTERISATION OF THE AIR TEMPERATURE FIELD ABOVE LARGE-FOOTPRINT BUILDINGS – FULL-SCALE EXPERIMENTS AND LARGE EDDY CFD SIMULATIONS

Alan Green[1], Riccardo Paolini[2], Afroditi Synnefa[2], Shamila Haddad[2], Paul Cooper[1], Mattheos Santamouris[2]

[1] Sustainable Buildings Research Centre, University of Wollongong, Wollongong, Australia

[2] Faculty of the Built Environment, University of New South Wales, Sydney, Australia

ABSTRACT

The implementation of 'cool' roofing materials, with high solar reflectance and infrared emittance, has received significant attention in recent years, as a method to mitigate the urban heat island effect and reduce building cooling energy requirements. The effect of 'cool' roofs on heat transfer through the roof structure has been investigated by many researchers. However, the air temperature field above roofs and the influence of elevated above-roof air temperatures on the performance of rooftop air-conditioning equipment and photovoltaic panels have not been studied in depth.

This paper describes detailed measurements that were taken in the thermal boundary layer above a large-footprint building. Air and roof surface temperatures were monitored at up to 63 locations above the roof of the building, and a comprehensive set of weather parameters were logged. Additional measurements were taken on specific days to characterise the atmospheric boundary layer profiles upwind of the building, measure air velocities above the roof, and determine the roof surface solar reflectance and infrared emittance. Roof surface temperatures were observed to often exceed the ambient air temperature by 30°C during the middle of the day. Air temperatures within 1.5m of the roof surface were typically 0.5-4°C above the ambient air temperature for several hours each day.

Computational Fluid Dynamics (CFD) simulation of convective heat transfer from building roofs is challenging, due to the complex urban geometries and high Reynolds numbers involved, and the wide range of relevant Richardson numbers, which span forced, mixed and natural convective regimes. Accurate simulation of thermal and velocity boundary layers is essential for such cases, but extremely fine computational grids are required to do so without the use of wall functions.

The ability of CFD simulations using wall functions to accurately model above-roof temperature fields was tested in the present work. Four CFD methods were compared, including delayed detached eddy simulations and wall-modelled large eddy simulations. Simulations of two cases, characterised by natural and mixed convection, were compared with results from the experimental campaign. The RMS deviation between simulated and measured air temperatures near the roof surface ranged from 0.74°C to 2.26°C. These discrepancies were of the same order of magnitude as the temperature differences that were of interest, which indicated that CFD methods involving wall functions may not be suitable tools for the investigation of above-roof temperature fields.

1 INTRODUCTION

1.1 COOL ROOFS AND ABOVE-ROOF AIR TEMPERATURE

Cool roofs are characterised by high solar reflectance and infrared emittance. The temperature of roof surfaces is highly dependent on these two properties [6]; 'cool' surfaces will absorb less heat from the sun than surfaces with lower solar reflectance and radiate more heat to their surroundings than surfaces with lower emittance. The inclusion of such surfaces in building envelopes can reduce the amount of heat transmitted into the building, and decrease the temperature of air in the outdoor environment.

Many previous studies have quantified the benefits of cool roofs, in terms of urban heat island mitigation and the reduction of annual building energy consumption (see, e.g., [14,25,28,31]). However, very few of these studies have addressed the effects of locally elevated air temperatures on rooftop heating, ventilation and air-conditioning (HVAC) equipment or photovoltaic (PV) panels. The efficiency of HVAC condenser units and PV panels

could be reduced significantly by high ambient temperatures, and the thermal load on HVAC systems may be increased significantly if ventilation air is drawn from within the above-roof thermal boundary layer. Such effects could be mitigated by the implementation of cool roofs.

Five previous investigations have attempted to quantify the effects of above-roof temperature on HVAC equipment, and the mitigation of such effects by cool roofs [9,10,19,26,33]. The methodologies adopted in these studies varied, as did the buildings, materials and rooftop equipment under investigation. Consequently, a wide range of results have been produced. On average, air temperatures measured near rooftop equipment in peak solar conditions have been between 0.3°C [33] and 3.5°C [10] hotter than reference 'ambient' measurements, taken further from the roof surfaces. Based on these results, estimated reductions in annual building energy demand due to the above-roof air temperature field have ranged from 0.3% [33] to 34.5% [9], in addition to the benefits of cool roofs predicted by conventional means (i.e. without taking local air temperature anomalies into account).

In addition to differences between the equipment, materials and buildings under investigation, inconsistencies in these previous results may be partially caused by methodological issues. For example, some outdoor temperature sensors in these studies were not shielded from solar radiation [26], computational fluid dynamics (CFD) techniques were applied without reference to relevant validation studies [10] and reference 'ambient' temperatures were measured relatively close to hot roof surfaces in some cases [33].

In the present study, experiments were conducted to produce a more comprehensive and rigorous evidence base, for investigation into the effects of the above-roof temperature field on the performance of rooftop equipment.

1.2 CFD SIMULATION OF ABOVE-ROOF AIR TEMPERATURE

The importance of validation in CFD studies has been outlined in many best-practice guidelines and scientific reviews (see, e.g., [4,7,15,30,32]). Previous comparisons between CFD simulations of heat transfer at building external surfaces and experimental results have exposed inherent flaws in some CFD techniques. Simulations based on the Reynolds-averaged Navier-Stokes (RANS) equations have not been able to accurately predict heat transfer at the top or side surfaces of buildings (i.e. those surfaces parallel with the mean wind direction) in several cases [11,21,22]. Turbulence-resolving techniques, such as wall-modelled large eddy simulation (WMLES) and delayed detached eddy simulation (DDES), have produced more accurate results in some cases [16,17,21,24]. However, even these more complex techniques have been shown to produce errors of approximately 40% in some simulations of heat transfer at building external surfaces [5,20,23].

The high Reynolds numbers (*Re*) encountered in urban flows pose an additional challenge to CFD practitioners. Many of the abovementioned validation studies have replicated wind-tunnel experiments, and therefore involved flows with *Re* several orders of magnitude smaller than those relevant to large buildings. In order to resolve boundary layers down to the viscous sub-layer at such high *Re*, the computational grid must have extremely fine resolution in the wall-normal direction at solid boundaries. The use of wall functions can alleviate requirements for a fine near-wall grid, but such models are not universally applicable in cases of heat transfer [5,12,13], so it is important that their influence on simulation accuracy be assessed when they are applied. Defraeye *et al.* [12] proposed a modified wall function, for simulations of heat transfer at building external surfaces. Its performance has been compared to RANS-based CFD simulations conducted without wall functions, for cases involving forced [12], mixed [13] and natural [1] convection. However, this approach does not appear to have yet been validated with experimental data.

A further complication in CFD simulations of urban thermodynamics is in establishing a method that will produce accurate results within the full range of Richardson numbers (*Ri*) relevant to the atmospheric boundary layer. Both stable and unstable stratification are often encountered in such flows, with forced, mixed and natural convection from surfaces exposed to the sun and sky. While several of the abovementioned validation studies went on to apply the tested CFD methods to flows involving natural and mixed convection, only one of the studies compared experimental results to simulations of mixed convection [5], and none validated a CFD methodology for simulating natural convection from buildings.

The accuracy of several CFD techniques has been compared in the present work, using cases taken from the experimental campaign. All of the techniques considered here involved the use of wall functions. Cases representing both mixed and natural convection were simulated.

2 METHODOLOGY

2.1 EXPERIMENTS

Experiments were conducted at a shopping centre, located in Nowra, New South Wales, Australia. The building had a 15,978m^2 aged, metal-coated steel roof (see Figure 1), which supported an array of PV panels and several rooftop HVAC units, including intakes for ventilation air, cooling towers and air-cooled heat exchangers.

The building was monitored for a period of 6 weeks, with measurements logged every 5 minutes. Fifteen 1.5m masts were installed on the roof (see Figure 2); each was fitted with four Hobo TMCX-HD thermistors, three were shielded from radiant heat transfer and fixed at heights of 0.15m, 0.5m and 1.5m above the roof surface, and one was adhered to the roof surface with a thermally conductive compound and shielded from radiative heat transfer by a small piece of aerogel insulation coated in foil tape. Air temperature, humidity, pressure, mean wind velocity and turbulence intensity were measured at the top of an 8m mast using a Gill MetPak Pro weather station (see Figure 2). Short-

wave and long-wave radiation exchange with the sun and sky were also monitored at the top of the mast, using a Middleton Solar EQ08-SE pyranometer and a Middleton Solar PG01-E pyrgeometer, respectively. Air temperatures were also measured 2m and 5m above the roof, using two platinum resistance temperature sensors which conformed to BS EN 60751:1995 class 1/3. Rainfall was monitored using a RIMCO-7499-STD tipping-bucket rain gauge.

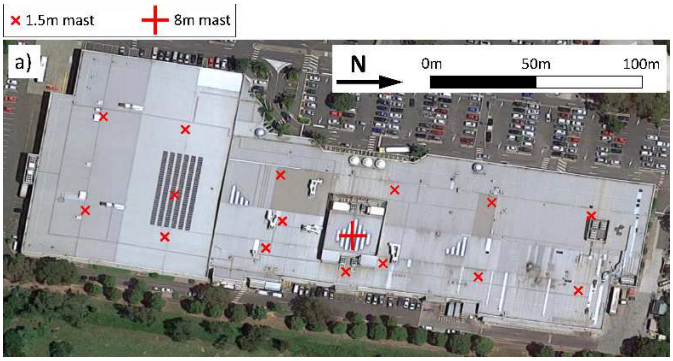

Figure 1: Aerial view of the case-study building. The locations of fixed monitoring equipment are indicated by the red crosses.

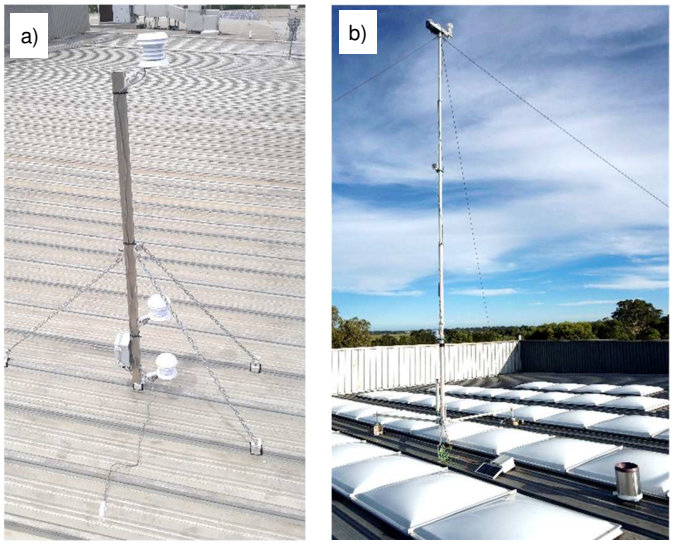

Figure 2: Equipment that was installed on the three roofs: a) one of the fifteen 1.5m masts, each of which was fitted with three shielded air temperature sensors and one surface temperature sensor; and b) the 8m mast, which was fitted with a weather station.

Additional, point-in-time measurements were taken during the 6-week monitoring period. A drone, fitted with a Workswell WIRIS 640 infrared camera, was used to take several hundred images of the building roof. The images were combined to form two thermal maps, from two different points in time. For several hours encompassing each drone flight, measurements were taken of the atmospheric boundary layer velocity and temperature profiles upwind of the building, as well as wind speeds and velocities close to the roof surface. Three Gill MetPak Pro weather stations were used to characterise the atmospheric boundary layer, by measuring temperature and horizontal air velocity at three heights. Two opposed Modern Device rev. P wind speed sensors were used to measure wind speed at the location of each 1.5m mast, at a height of 1m above the roof surface and at a rate of 1Hz. Three-dimensional air velocities were also measured at two locations above the roof during these periods, at a rate of 20Hz, using Gill Windmaster anemometers. The solar reflectance of the roof surface was measured at six locations using an albedometer (NR01 net radiometer by Hukseflux) according to ASTM E 1918 [3]. The roof thermal emittance was measured using a portable Devices & Services emissometer according to ASTM C 1371 [2] and, additionally, by matching the surface temperatures measured by the thermistors attached to the roof surface to those measured using a T540 by FLIR thermal camera.

2.2 CFD SIMULATIONS

Two test cases were established, corresponding to conditions when the point-in-time measurements had been taken. Of the two cases, one was within the natural convective regime, with $Re \approx 1\times10^7$, $Ri \approx 48.7$, and the other was within the mixed convective regime, with $Re \approx 4.2\times10^7$, $Ri \approx 1.59$; here, Re and Ri are based on a representative building wall length of 100m. Both cases were treated as quasi-steady. CFD simulations corresponding to each case were run using the software ANSYS Fluent 18.2, in a computational domain containing a simplified version of the Nowra building geometry (see Figure 3). The domain dimensions were set such that the blockage ratio due to the building geometry was less than 3%.

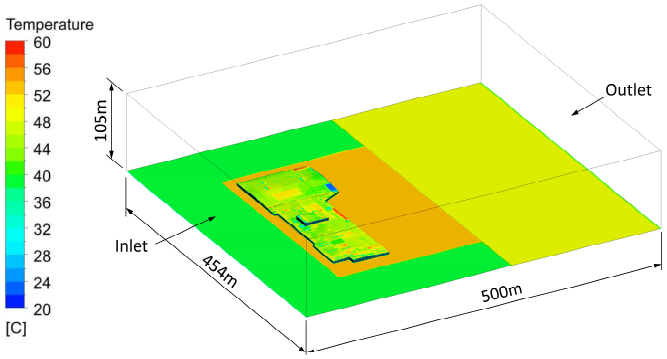

Figure 3: Computational domain used for CFD simulations of the Nowra building. Solid boundaries have been coloured according to the constant temperature fixed at these surfaces in the mixed-convection case.

Non-conformal computational grids were formed in the domain, using a cut-cell method. Iousef, *et al.* [17] have shown that cases similar to those considered here can be simulated accurately using non-conformal grids, despite the abrupt changes in grid spacing that they exhibit. The distance from solid boundaries to the centre of the nearest computational cell was fixed at 5mm, which gave dimensionless wall distances, often referred to as y^+, of approximately 35 and 100 in the natural and mixed convection cases, respectively. Fine, medium and coarse versions of the grid were generated, for use in a grid sensitivity

analysis. A refinement ratio of 1.5 was used in each dimension, resulting in grids with between 4.8×10^6 and 15.8×10^6 elements.

Simulations were run using: a) the incompressible steady RANS equations with the realisable k-ε turbulence model and scalable wall functions [18], b) the incompressible steady RANS equations with the realisable k-ε turbulence model and wall functions modified according to [12], c) DDES with the realisable k-ε turbulence model and scalable wall functions, and d) WMLES, according to the formulation proposed in [29]. Buoyancy effects were included in all simulations using the Boussinesq approximation.

Boundary conditions were set corresponding to the two test cases. The aerodynamic terrain roughness was determined from field measurements and used to define logarithmic mean velocity profiles [27], which were fixed at the domain inlet (see Figure 4). The mean wind direction in both cases was within 5° of being normal to the building eastern wall, so all simulations were run with this wind direction. The inlet air temperature for each case was also defined using a logarithmic profile, which was fitted to the experimental data (see Figure 4). In simulations using DDES and WMLES, the vortex method was used to superimpose synthetic eddies over the mean inlet flow.

Solid surfaces within the domain were assigned representative aerodynamic roughness and constant temperature boundary conditions, except for the walls of the building, which were set as adiabatic. Temperatures from the aerial infrared photographs were mapped onto the building roof, and average temperatures from the photographs were assigned to three ground regions surrounding the building, corresponding to the grass-covered area upwind of the building, the carpark and service road immediately surrounding the building and the suburban area downwind of the building (see Figure 3). 'Symmetry' boundary conditions (i.e. zero flux of all quantities) were fixed at the lateral boundaries, the static pressure at the outlet was fixed and the top boundary was set with the same fixed velocity and temperature as the top of the inlet.

The coupled pressure-based solver was used, with least-squares cell-based spatial discretisation of gradients and second order discretisation of advection terms in all governing equations. DDES and WMLES were conducted with time-steps of 0.04s, which kept the cell courant number below 1. These transient simulations were initialised with the RANS-based solutions, allowed to run until the flows reached quasi-steady states, then run and sampled until the time-averaged results stabilised.

Initial trial simulations were conducted in a long, empty two-dimensional domain, with a similar grid spacing and boundary conditions to those that were used for the final simulations. Results from these trials were checked to ensure that the grid and boundary conditions produced a horizontally homogeneous atmospheric boundary layer. A grid sensitivity analysis was also conducted, to ensure that grid-induced errors were acceptably low. Simulated air temperatures and velocities near the roof surface were compared to those measured during the experimental campaign.

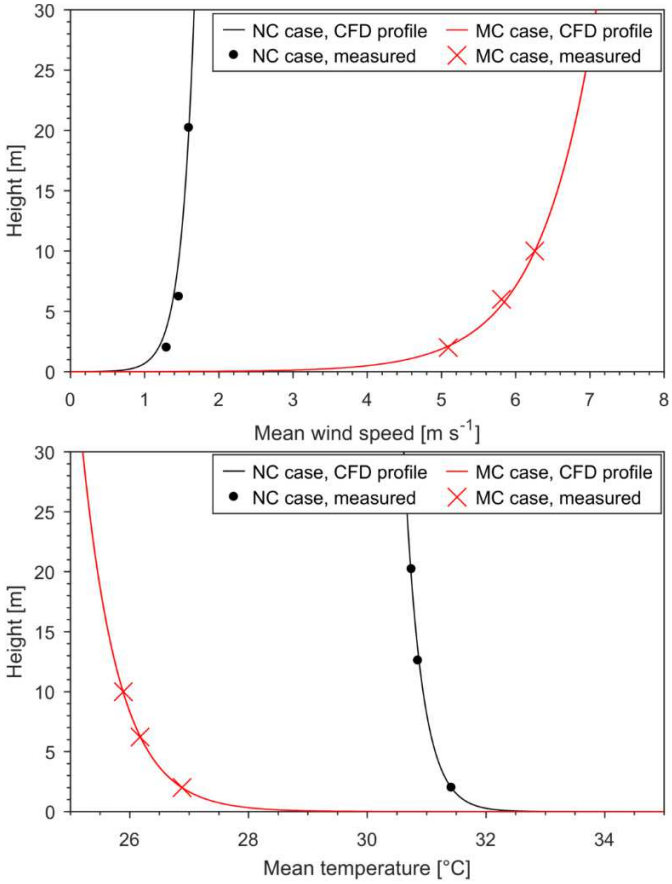

Figure 4: Vertical profiles of mean wind velocity (top) and mean air temperature (bottom) from the natural convection (NC) case and mixed convection (MC) case, which were imposed at the domain inlet during computational fluid dynamics (CFD) simulations.

3 RESULTS AND DISCUSSION

3.1 ROOF SURFACE PROPERTIES

The roof surface solar reflectance measurements ranged from 0.21 to 0.29, with a mean of 0.27. Measurements taken with the emissometer and thermal camera indicated that the roof surface thermal emittance was approximately 0.625. Such properties are commensurate with previous measurements of aged metal-coated steel roofs.

3.2 REFERENCE AMBIENT TEMPERATURE

Definition of one representative 'ambient' temperature in a spatially variable atmospheric temperature field is somewhat arbitrary. However, such a definition is necessary, since it allows the temperature elevation close to a roof surface to be quantified. The Australian Bureau of Meteorology (BOM) defines the 'ambient' air temperature as that which is measured at a height of 1.1m over a flat, grass-covered area [8]. Since it was not possible to install equipment at such a site close to the case study

building, it was necessary to define an alternative local reference temperature.

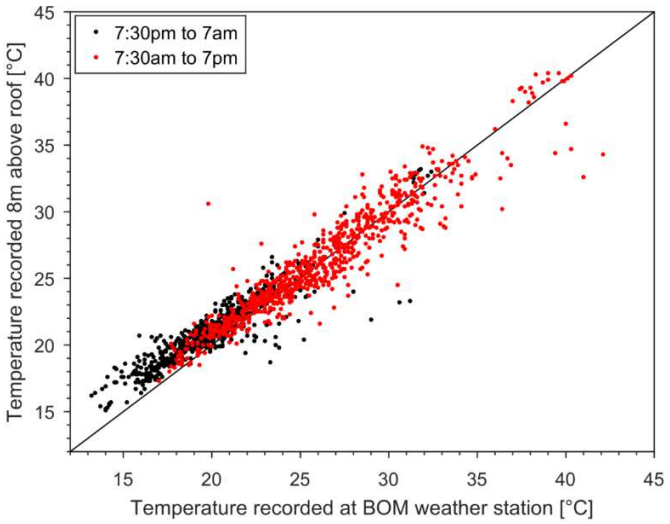

Figure 5: Comparison between air temperatures measured 8m above the roof and those measured at a Bureau of Meteorology (BOM) weather station, approximately 9km from the building.

Comparison of temperatures measured 8m above the building roof and those measured at the nearest BOM weather station revealed that the former set of measurements were likely to represent the local 'ambient' temperature well. Daytime temperature measurements were very similar on-average, and typically differed by less than 3°C (see Figure 5). The night-time measurements taken 8m above the building tended to be 0–3°C warmer than the corresponding BOM measurements. The difference in mean night-time temperature may have been partially due to an urban heat island effect, since the building was at the edge of a suburban area while the BOM weather station was located at an air strip, surrounded by forest. Differences in the heights at which the measurements were taken may have also contributed to a discrepancy in night-time measurements, since stable atmospheric stratification is common at night-time and the mast-mounted sensor was approximately 16m higher from the ground than the BOM sensor was. In the proceeding analysis, temperature measurements taken at the top of the 8m mast have been used as the reference 'ambient' temperature.

3.3 ROOF SURFACE TEMPERATURE

Roof surface temperatures, measured using the fifteen 1.5m masts and the drone-mounted infrared camera, demonstrated that conventional (i.e. 'non-cool') roof surfaces can reach temperatures more than 50°C above 'ambient' (see Figure 6 and Figure 7). The mean roof surface temperature elevation measured between 12:30 and 13:30, over the entire 6-week monitoring period, was 28.2°C.

3.4 ABOVE-ROOF AIR TEMPERATURE

Air temperatures measured close to the roof surface were typically 0.5–4°C hotter than reference 'ambient' temperatures during the middle of the day, i.e. from 10:00 to 16:00 (see Figure 8). Night-time measurements were typically 0–1.5°C colder than the reference 'ambient' temperature. These values represent the degree to which conventional building simulation practices may misrepresent the 'ambient' air temperature surrounding rooftop HVAC equipment and PV panels.

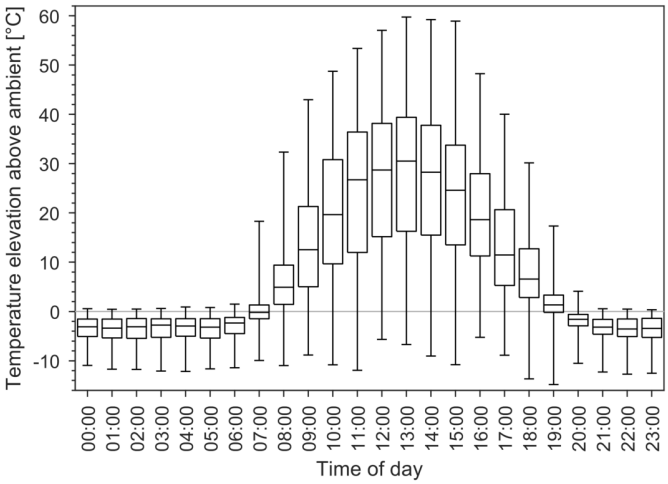

Figure 6: Measured temperature differences between the roof surface and reference 'ambient' air temperatures. These distributions include all surface temperatures measured by the fifteen 1.5m masts on the Nowra building during the 6 week monitoring period.

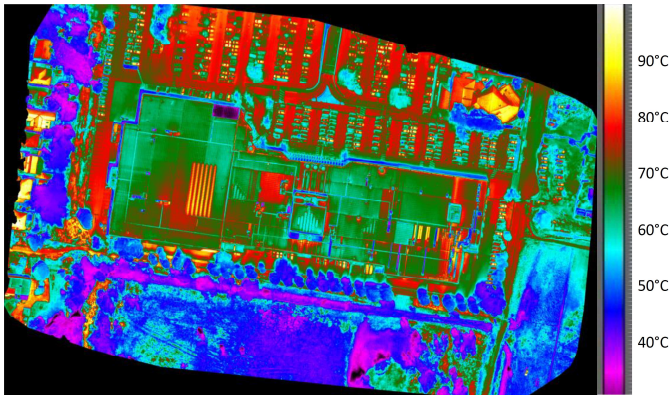

Figure 7: Thermal image of the Nowra roof and surrounding area, taken from above. This image was captured at the point in time that was used as the natural convection case for CFD simulations.

A vertical temperature gradient was consistently resolved in the air temperature measurements taken close to the roof surface. The thermal boundary layer thickness, defined here as the distance from the roof at which the difference between the local air temperature and reference 'ambient' temperature equalled 5% of the difference between the local roof surface temperature and the reference 'ambient' temperature, was typically in the order of 150mm during periods of unstable stratification, and slightly greater than 1.5m when air above the roofs was stably stratified.

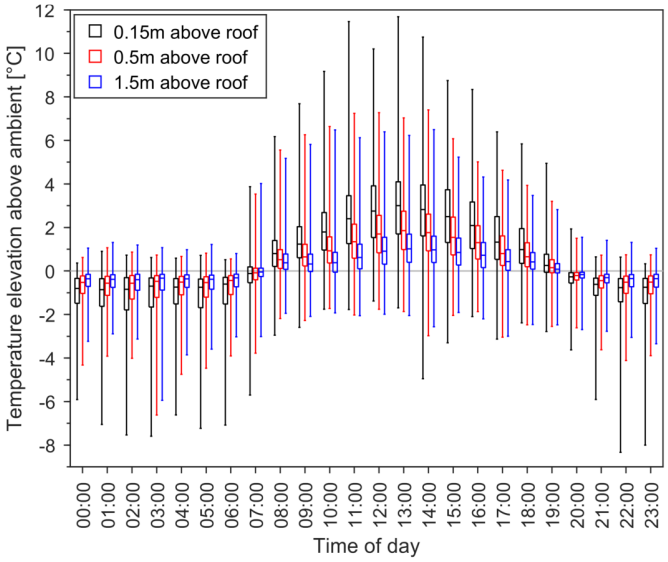

Figure 8: Measured temperature differences between sensors close to the roof surface and reference 'ambient' air temperatures. These distributions include all air temperatures measured by the fifteen 1.5m masts on the Nowra building during the 6 week monitoring period.

3.5 UNCERTAINTY IN TEMPERATURE MEASUREMENTS

The accuracy of temperature sensors and data logging equipment used in the present study was confirmed to be within ±0.1°C, using a high-precision thermal bath and traceable reference thermometers. However, direct and reflected solar radiation can adversely affect outdoor air and surface temperature measurements, even when sensors are shielded as they were in the present work. The overall uncertainty in temperature measurements obtained during the daytime and night-time were estimated to be ±0.7°C and ±0.3°C, respectively.

3.6 COMPARISON OF CFD METHODS

Significant differences were observed between the outputs of the four CFD methods that were tested (see Figure 9). In the natural convection case, near-roof air temperatures were under-predicted by all methods except RANS with modified wall functions. In that case, the root-mean squared (RMS) deviation between CFD and experimental results ranged from 1.25°C (RANS with modified wall functions) to 2.26°C (WMLES). Simulations of the mixed convection case were generally in closer agreement with experimental results, with RMS deviations of 0.74°C (RANS, DDES and WMLES) and 1.51°C (RANS with modified wall functions). However, inaccuracies of such a magnitude are significant in investigations concerned with temperature differences in the order of 1°C.

The primary differences between the four CFD methods tested here were: a) DDES and WMLES simulated transient flow, while the RANS-based methods produced a time-averaged result directly; b) DDES and WMLES explicitly resolved large turbulent eddies away from solid boundaries, and thus relied less on models to predict turbulent diffusion than the RANS-based methods did; c) turbulence could be resolved closer to solid boundaries in WMLES than it could in DDES; d) WMLES used a single-equation turbulence model close to solid boundaries, while the other three methods used the two-equation realisable k-ε turbulence model; and e) the modified wall function utilised a larger turbulent Prandtl number than the standard wall function. In terms of these important differences, several observations can be made:

- The transient, turbulence-resolving methods did produce different near-roof air temperatures than RANS, but the RMS deviation from experimental results was not improved in the mixed convection case.
- In the natural convection case, the one-equation turbulence model, implemented near walls in WMLES, did not predict near-roof temperatures as well as the two-equation model implemented in DDES.
- The wall function modification proposed by Defraeye, Blocken and Carmeliet (2011) produced significantly higher near-roof air temperatures than standard wall functions. In the mixed convection case, this increased the difference between CFD and experimental results significantly.

4 CONCLUSION

Experiments have been conducted on a large-footprint building, which involved detailed measurements throughout the thermal boundary layer above the building roof. The roof surface typically reached temperatures 30°C above the 'ambient' air temperature in the middle of the day, and exceeded 'ambient' temperatures by more than 50°C on some days during the 6 week monitoring period. Night-time roof surface temperatures were 3°C lower than 'ambient' temperatures, on average. A vertical temperature gradient was consistently observed above the roof surface, with a thermal boundary layer depth in the order of 150mm and 1.5m at times of unstable and stable stratification, respectively.

Air temperatures surrounding rooftop HVAC equipment and PV panels were often measured to be 0.5–4°C above 'ambient' in the middle of the day. Such local temperature anomalies are typically not taken into account in predictions of building energy performance, and could have a significant effect on results if they were. The value proposition of 'cool' roofing materials, in particular, could be different to previous estimations that neglected the effects of the near-roof temperature field, since these products are likely to mitigate such effects.

It appears that CFD simulations adopting the methods tested in the present study are not suitable for investigations of natural convection from building roofs. Better agreement was observed between CFD and experimental results in the mixed convection case, but the deviations that were observed were still significant, given that temperature differences in the order of 1°C were of interest. The RMS deviation between simulated and measured near-roof air temperatures ranged from 0.74°C to 2.26°C. It is possible that CFD can produce more accurate results when a finer near-wall grid is used, in order to avoid the use of wall functions.

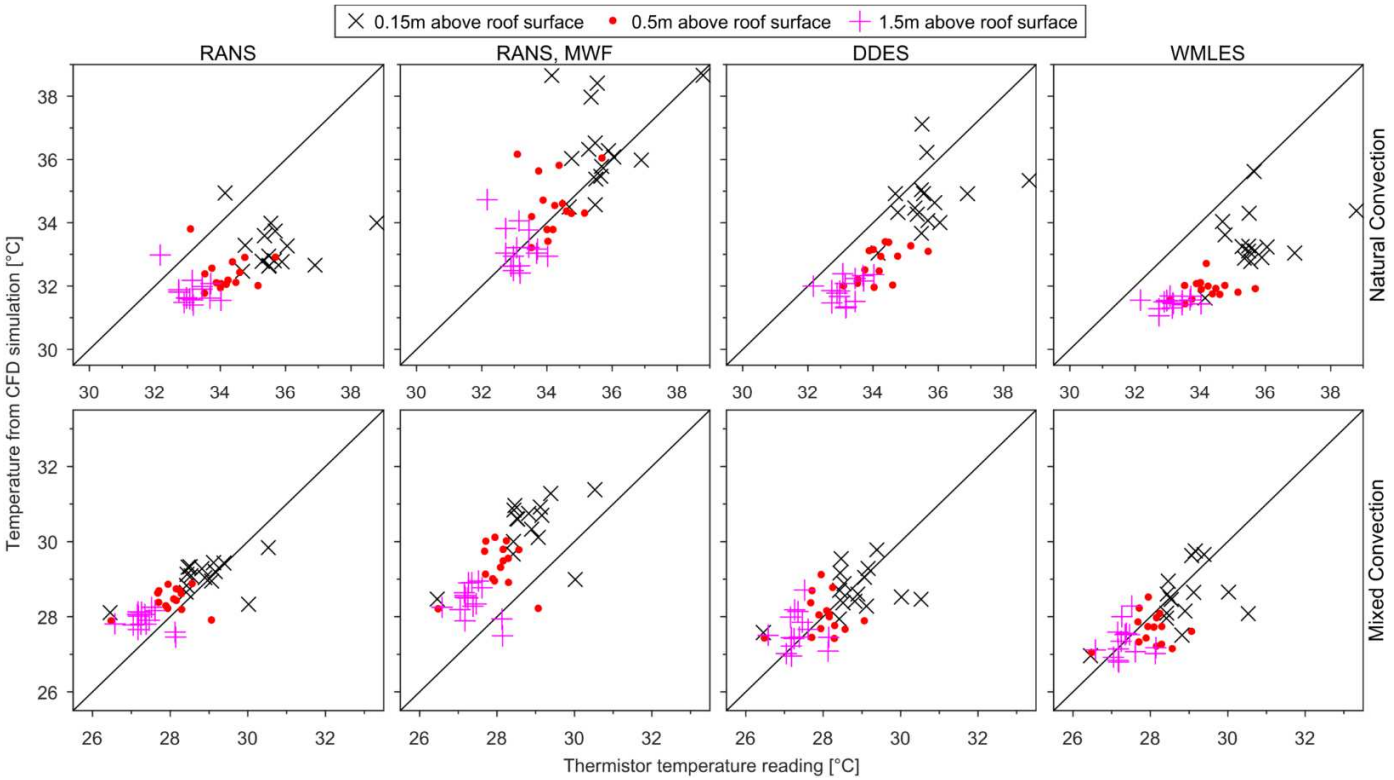

Figure 9: Comparison of experimental results with air temperatures simulated close to the Nowra roof, in the natural convection case (top) and mixed convection case (bottom), using RANS-based simulations with standard wall functions (left), RANS-based simulations with modified wall functions (MWF; centre-left), DDES (centre-right) and WMLES (right).

Further work was ongoing at the time of writing, including experiments at two other buildings and the comparison of results presented here to CFD simulations conducted without wall functions. Work has also been planned to quantify the effects of the measured above-roof temperatures on rooftop HVAC equipment and PV panels, and the effects of such effects on the value proposition of 'cool' roofing products.

NOMENCLATURE

Re – Reynolds number, based on a representative building wall length of 100m and the mean wind velocity at a height of 10m.

Ri – Richardson number, defined using the difference between the average roof surface temperature and the reference 'ambient' air temperature.

y^+ – Dimensionless wall distance in CFD simulations, equal to the distance to the nearest wall, multiplied by friction velocity at the wall and divided by the kinematic viscosity.

ACKNOWLEDGMENTS

This research is funded by the CRC for Low Carbon Living Ltd supported by the Cooperative Research Centres program, an Australian Government initiative. The authors would also like to acknowledge BlueScope Steel and Stockland, for their collaboration on the research.

REFERENCES

[1] Allegrini, J. et al., An Adaptive Temperature Wall Function for Mixed Convective Flows at Exterior Surfaces of Buildings in Street Canyons, *Building and Environment*, **49**(0), 2012, 55-66.

[2] ASTM, ASTM C 1371: Standard Test Method for Determination of Emittance of Materials near Room Temperature Using Portable Emissometers, American Society for Testing and Materials, West Conshohocken, PA, 2015.

[3] ASTM, ASTM E 1918: Standard Test Method for Measuring Solar Reflectance of Horizontal and Low-Sloped Surfaces in the Field, American Society for Testing and Materials, West Conshohocken, PA, 2016.

[4] Blocken, B., 50 Years of Computational Wind Engineering: Past, Present and Future, *Journal of Wind Engineering and Industrial Aerodynamics*, **129**(0), 2014, 69-102.

[5] Boppana, V., Xie, Z.-T. & Castro, I.P., Large-Eddy Simulation of Heat Transfer from a Single Cube Mounted on a Very Rough Wall, *Boundary-layer meteorology*, **147**(3), 2013, 347-368.

[6] Bretz, S.E. & Akbari, H., Long-Term Performance of High-Albedo Roof Coatings, *Energy and buildings*, **25**(2), 1997, 159-167.

[7] Britter, R. & Schatzmann, M., Model Evaluation Guidance and Protocol Document, European Cooperation in Sciences and Technology, COST Office Brussels, 2007.

[8] Canterford, R., Observation Specification No. 2013.1, Bureau of Meteorology, Department of the Environment, Sports and Territories, 1997.

[9] Carter, G., Issues and Solutions to More Realistically Simulate Conventional and Cool Roofs, in *Proceedings of Building Simulation 2011: 12th Conference of international building performance simulation association (IBPSA). Sydney, 14–16 November 2011*, 2011.

[10] Carter, G. & Kosasih, B., Not So Cool Roofs, in *AIRAH's Future of HVAC 2015 Conference*, Melbourne, Australia, 2015.

[11] Defraeye, T., Blocken, B. & Carmeliet, J., CFD Analysis of Convective Heat Transfer at the Surfaces of a Cube Immersed in a Turbulent Boundary Layer, *International Journal of Heat and Mass Transfer*, **53**(1), 2010, 297-308.

[12] Defraeye, T., Blocken, B. & Carmeliet, J., An Adjusted Temperature Wall Function for Turbulent Forced Convective Heat Transfer for Bluff Bodies in the Atmospheric Boundary Layer, *Building and Environment*, **46**(11), 2011, 2130-2141.

[13] Defraeye, T., Blocken, B. & Carmeliet, J., Cfd Simulation of Heat Transfer at Surfaces of Bluff Bodies in Turbulent Boundary Layers: Evaluation of a Forced-Convective Temperature Wall Function for Mixed Convection, *Journal of Wind Engineering and Industrial Aerodynamics*, **104**, 2012, 439-446.

[14] EPA, Reducing Urban Heat Islands: Compendium of Strategies - Cool Roofs, 2014.

[15] Franke, J. et al., *Best Practice Guideline for the CFD Simulation of Flows in the Urban Environment*, 2007.

[16] Hu, Z.-X., Cui, G.-X. & Zhang, Z.-S., Numerical Study of Mixed Convective Heat Transfer Coefficients for Building Cluster, *Journal of Wind Engineering and Industrial Aerodynamics*, **172**, 2018, 170-180.

[17] Iousef, S. et al., On the Use of Non-Conformal Grids for Economic Les of Wind Flow and Convective Heat Transfer for a Wall-Mounted Cube, *Building and Environment*, **119**, 2017, 44-61.

[18] Launder, B.E. & Spalding, D.B., The Numerical Computation of Turbulent Flows, *Computer methods in applied mechanics and engineering*, **3**(2), 1974, 269-289.

[19] Leonard, T. & Leonard, T. Stay Cool: A Roof System on a Minnesota Building Demonstrates Energy-Saving Technology. Professional Roofing, 2006.

[20] Li, Q. et al., Quality and Reliability of Les of Convective Scalar Transfer at High Reynolds Numbers, *International Journal of Heat and Mass Transfer*, **102**, 2016, 959-970.

[21] Liu, J., Srebric, J. & Yu, N., Numerical Simulation of Convective Heat Transfer Coefficients at the External Surfaces of Building Arrays Immersed in a Turbulent Boundary Layer, *International Journal of Heat and Mass Transfer*, **61**(0), 2013, 209-225.

[22] Montazeri, H. & Blocken, B., New Generalized Expressions for Forced Convective Heat Transfer Coefficients at Building Facades and Roofs, *Building and Environment*, **119**, 2017, 153-168.

[23] Nazarian, N. & Kleissl, J., Realistic Solar Heating in Urban Areas: Air Exchange and Street-Canyon Ventilation, *Building and Environment*, **95**, 2016, 75-93.

[24] Ničeno, B., Dronkers, A.D.T. & Hanjalić, K., Turbulent Heat Transfer from a Multi-Layered Wall-Mounted Cube Matrix: A Large Eddy Simulation, *International Journal of Heat and Fluid Flow*, **23**(2), 2002, 173-185.

[25] Pisello, A.L., State of the Art on the Development of Cool Coatings for Buildings and Cities, *Solar Energy*, **144**, 2017, 660-680.

[26] Pisello, A.L., Santamouris, M. & Cotana, F., Active Cool Roof Effect: Impact of Cool Roofs on Cooling System Efficiency, *Advances in building energy research*, **7**(2), 2013, 209-221.

[27] Richards, P.J. & Norris, S.E., Appropriate Boundary Conditions for Computational Wind Engineering Models Revisited, *Journal of Wind Engineering and Industrial Aerodynamics*, **99**(4), 2011, 257-266.

[28] Santamouris, M., Synnefa, A. & Karlessi, T., Using Advanced Cool Materials in the Urban Built Environment to Mitigate Heat Islands and Improve Thermal Comfort Conditions, *Solar Energy*, **85**(12), 2011, 3085-3102.

[29] Shur, M.L. et al., A Hybrid Rans-Les Approach with Delayed-Des and Wall-Modelled Les Capabilities, *International Journal of Heat and Fluid Flow*, **29**(6), 2008, 1638-1649.

[30] Stathopoulos, T., The Numerical Wind Tunnel for Industrial Aerodynamics: Real or Virtual in the New Millennium?, *Wind and Structures*, **5**(2), 2002, 193-208.

[31] Synnefa, A. & Santamouris, M., Chapter 4: Mitigating the Urban Heat with Cool Materials for the Buildings' Fabric, in *Urban Climate Mitigation Techniques*, editors M. Santamouris and D. Kolokotsa, Taylor and Francis, 2015, 67.

[32] Tominaga, Y. & Stathopoulos, T., Cfd Simulation of near-Field Pollutant Dispersion in the Urban Environment: A Review of Current Modeling Techniques, *Atmospheric Environment*, **79**(0), 2013, 716-730.

[33] Wray, C. & Akbari, H., The Effects of Roof Reflectance on Air Temperatures Surrounding a Rooftop Condensing Unit, *Energy and Buildings*, **40**(1), 2008, 11-28.